Design Consideration of Parallel–Parallel Connected Piezoelectric Transformer for Thermal Balance

Japanese Journal of Applied Physics
Vol. 46, No. 10B, 2007, pp. 7067–7072

Design Consideration of Parallel–Parallel Connected Piezoelectric Transformer for Thermal Balance

Joung-Hu PARK*, Sang-Min LEE, Sung-Jin CHOI, and Bo-Hyung CHO

Power Electronics System Laboratory, Seoul National University, Seoul 151-744, Korea

(Received May 14, 2007; accepted July 2, 2007; published online October 22, 2007)

Recently, the multiple-connected piezoelectric transformer (PT) is considered as significant research topic especially for power processing applications. However, there is a power balance issues closely related to thermal failure of PT. To avoid the thermal imbalance between PTs, a design specification of thermal characteristic parameters of piezoelectric transformer in input-parallel and output-parallel connection has been presented. In first, the individual thermal characteristics of radial-vibration mode PTs are investigated and the results are also the required design area of thermal parameters in parallel–parallel connection by three steps. As an objective function, relative power-loss rate was defined and used for deriving the thermal balance design criteria. The design specification of major design parameters such as thermal parameter variation (ΔL_{eq}, ΔR_m), initial deviation of the variation (δL_{eqT}, δR_{mT}), and initial deviation of thermal parameters (δL_{eq0}, δR_{m0}) have been proposed as $(-0.002, -0.006)$, $(\pm 0.0001, \pm 0.0003)$, and $(\pm 0.0002, \pm 0.0004)$ respectively, and the analysis has been verified by the simulation results. [DOI: 10.1143/JJAP.46.7067]

KEYWORDS: piezoelectric transformer, multiple-connection, thermal balance, power balance, parallel–parallel

1. Introduction

Recently, some power device industries have been interested in piezoelectric transformer (PT) as a potential alternative for power processing applications such as power converter, lamp ballast, and so on.[1–3] However, single layer PT has a limitation of power capacity to handle with good efficiency and stable thermal-characteristics. For solving the problem, multiple-connected and multi-layer piezoelectric transformer structure is introduced for power processing applications. However, there is still a problem such that the thermal imbalance between the employed PTs can occur due to the deviation of electrically equivalent parameter values of PTs which have variation according to the thermal excitation. If the patterns of parameter variation or parameter deviation (device tolerance) are examined and controlled, the thermal imbalance problem can be relieved. Therefore, it is significant to suggest PT specification of the temperature variation parameter for thermally stable design of the multiple-connected PT applications. This paper presents the PT's thermal variation specifications of electrically equivalent parameters in input-parallel and output-parallel (parallel–parallel) connected PT structure, one of mostly-used conventional approaches.

Figure 1 shows the structure of multi-layered disk-type PT sample used in this research. The primary electrodes are located in the center part and the secondary one with multiple layers are concentrically arranged in the outer part of the disk and spaced from the primary electrodes.[4] The disk is polarized perpendicular to the plane of the electrodes, axial direction.[4] The PT is made of DIT D140, a hard ceramic material (PZT-4 series) with the characteristics shown in Table I. Advantages of the PTs are low profile and high isolation voltage rating, which is very suitable for the AC–DC/DC–DC switching power converter applications.[5] However, the PT can be significantly over-excited due to the thermal imbalance when multiple PT structures are employed. This over-excitement causes abnormal operations in the PT. Figure 2 shows the thermal distribution of the piezoelectric transformer measured by the universal thermal imager the part number IRI1001E (manufactured by IRISYS). The primary electrodes are the hottest point where the soldered joints can be over-heated and the connection wires can be detached by mechanical vibration when thermal imbalance becomes severe.

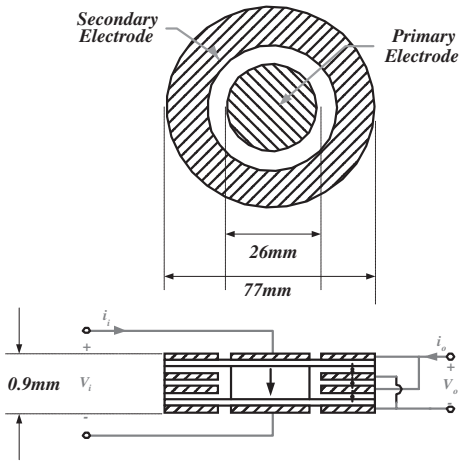

Fig. 1. Radial vibration mode PT structure.[4]

Table I. Parameter values of low-temperature-firing material, DIT D140.[3]

Coupling coefficient, k_p	0.60
Dielectric loss, $\tan\delta$	0.003
Relative dielectric constant, $\varepsilon_{33}^{T}/\varepsilon_0$	1500
Piezoelectric constant, d_{33} (C/N)	380×10^{-12}
Quality factor, Q_m	800
Temperature coefficient of cap. at 25–100 °C (ppm/°C)	3000

Figure 3 shows the thermal-imbalance temperature trajectory of 20 W radial vibration mode PTs (samples #2 and #5, arbitrary samples in a vibration-mode PT group of the same design) in parallel–parallel connection (measured by Mobile Corder MV200, Yokogawa). The parameter devia-

*E-mail address: whoishe@snu.ac.kr

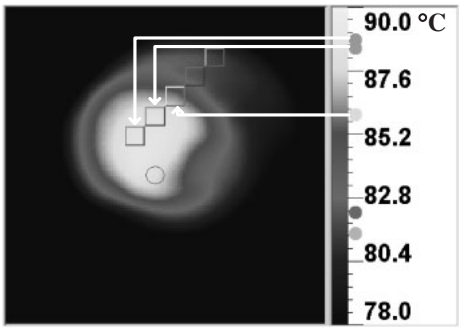

Fig. 2. Thermal distribution image of the excited PT.

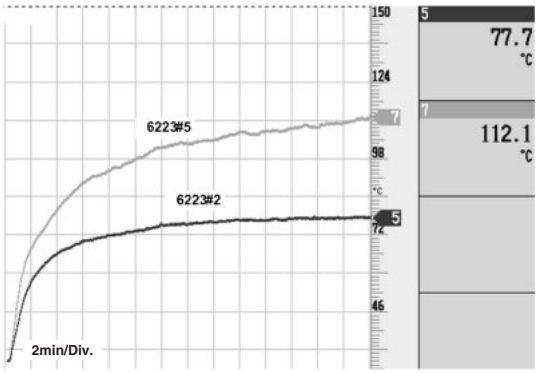

Fig. 3. Temperature trajectories of two PTs (samples #2 and #5, arbitrary samples in the same vibration-mode PT group) in parallel–parallel connection.[5)]

tions to each other are shown in Figs. 5 and 6. The output load was set to $R_{eq} = 25\,\Omega$ for the optimal load condition of the PTs. PT #5 rises up to 112 °C even before it reaches the steady-state, while the other PT #2 is still staying under 80 °C. The thermal imbalance effect among PTs should be removed when a power converter is designed with multiple-connected PTs. From the following section, thermal characteristics of disk-type PT will be investigated and the design guideline of the PT will also be included.

2. Thermal Characteristics of Piezoelectric Transformer in Power Applications

In this section, thermal characteristics of radial-vibration mode PTs will be considered by thermal variation of the equivalent parameters of electrical circuit model according to the temperature rise. It has been known that the rise causes some variation of material constants consisting in the PT body.[5–7)]

This phenomenon makes effects on the parameters of electrically-equivalent model, changing them from the initial values at room temperature. Therefore, the observation of the parameter variation is required to analyze the multiple-PT thermal balance. Figure 4 shows the electrically-equivalent circuit model of parallel–parallel PTs.[8,9)] In the figure, L_{eq} is equivalent inductance (impedance) to the impedance of the resonant branch at switching frequency, which is determined by:

$$L_{eq} = Z_r\left(\frac{1}{\omega_r} - \frac{\omega_r}{\omega_s^2}\right),$$

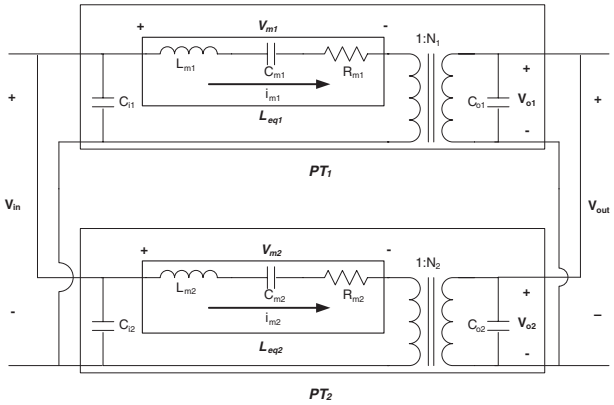

Fig. 4. The equivalent circuit model of two piezoelectric transformer in parallel–parallel connection.

$$Z_r = \sqrt{\frac{L_m}{C_m}},$$
$$\omega_r = \frac{1}{\sqrt{L_m C_m}}, \quad (1)$$

where, ω_s is switching frequency. The parameters according to the temperature-rise were observed with Network analyzer (HP4194) applying Admittance circle method. PTs were heated and cooled down repeatedly during the measuring process. The parameter variation curves are shown in Fig. 5. Figure 5 means the normalized variation-rates of the parameters at room temperature. All the parameters are ralative values divided by that of the ambient temperature. In Fig. 5, the curves look very similar each other in spite of the existence of absolute value deviation, sample by sample. In other words, it is shown that the input and output capacitances as well as the series capacitance in mechanical resonant branch increase, and the R and L of the branch decrease. On the other hand, turn ratio N has no difference in spite of the temperature rise.

Thermal parameters of the normalized variation rate (slope of the curve, $^\circ C^{-1}$) in Fig. 5 are defined as ΔC_i, ΔC_o, ΔL_{eq}, ΔR_m (input, output capacitance, L_{eq}, damping resistor). The turn-ratio N is not considered due to the invariance.

Based on these parameters, curves of the resonant frequency and the characteristic impedance are derived as shown in Fig. 6. The figure shows that all the frequencies of the PTs stays at an almost constant level and the characteristic impedance are downward with the temperature-rise.

3. Thermal Balance Analysis of Multiple-Connected PTs

Input-parallel and output-parallel connection is one of the most widely-used structure for the easy extension of power-capacity without redesign of PTs to satisfy the new optimal condition.

From eq. (1), it is shown that mechanical branch impedance Z_m is dependant on the characteristic impedance Z_r decreasing with temperature-rise. This temperature characteristic of L_{eq} is almost the same as the characteristic impedance Z_m, since the resonant frequency moves negligibly according to the data in Fig. 6 (ω_r is constant). The relationship is described as: $Z_m \approx sL_{eq}$.

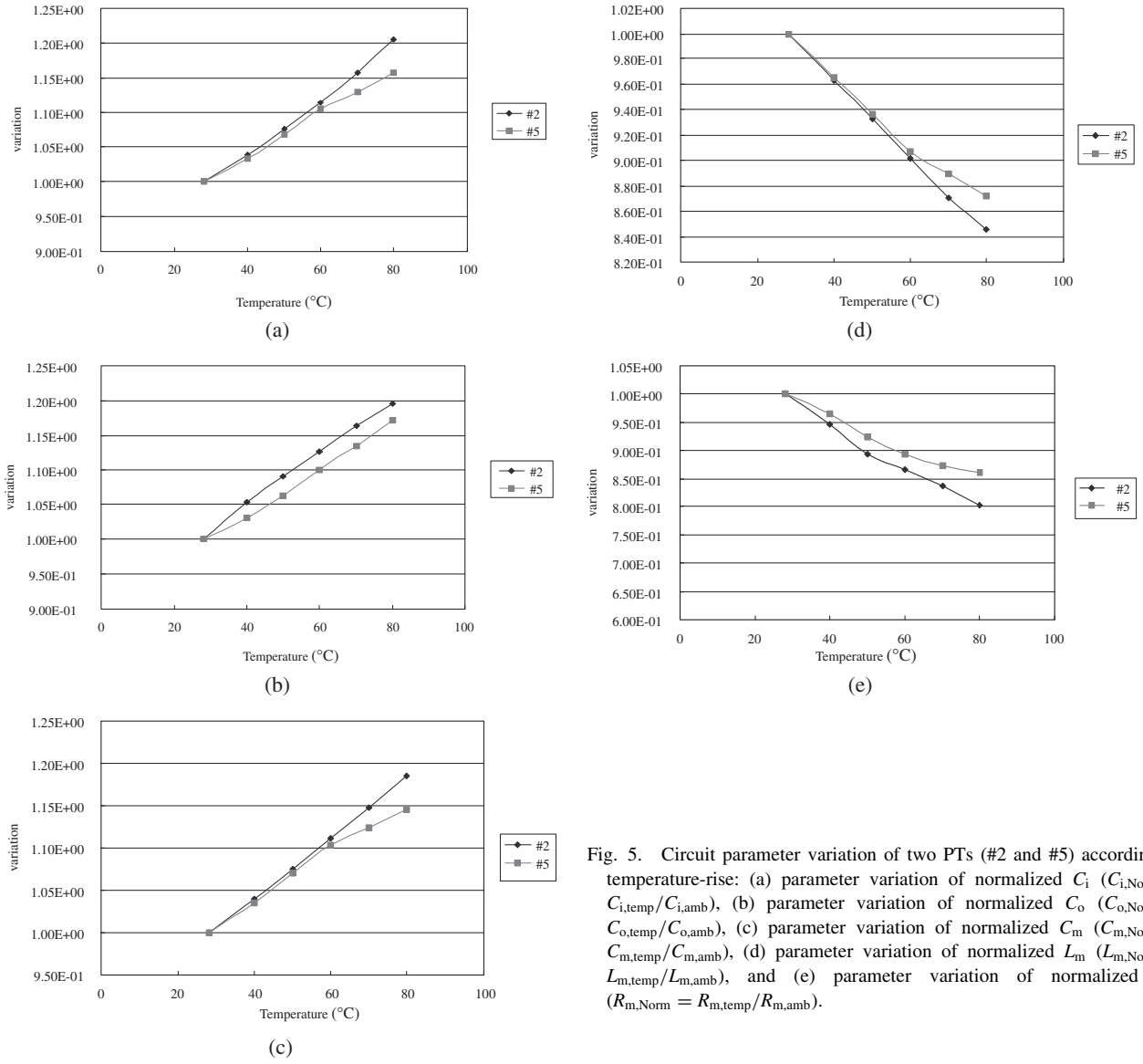

Fig. 5. Circuit parameter variation of two PTs (#2 and #5) according to temperature-rise: (a) parameter variation of normalized C_i ($C_{i,Norm} = C_{i,temp}/C_{i,amb}$), (b) parameter variation of normalized C_o ($C_{o,Norm} = C_{o,temp}/C_{o,amb}$), (c) parameter variation of normalized C_m ($C_{m,Norm} = C_{m,temp}/C_{m,amb}$), (d) parameter variation of normalized L_m ($L_{m,Norm} = L_{m,temp}/L_{m,amb}$), and (e) parameter variation of normalized R_m ($R_{m,Norm} = R_{m,temp}/R_{m,amb}$).

From the following section, analyze the thermal effect of multiple PTs, using L_{eq} characteristics.

3.1 PT Design specification of parameter variation rate according to thermal effect

From the circuit model, it is known that the mechanical loss by damping resistor R_m is the most dominant factor determining PT temperature. Therefore, it is feasible to estimate the thermal behavior by considering the power loss in each PT. Since the temperature of each PT is not the same through all the operating conditions in practical, with an assumption that a PT is hotter than the other, the relative power loss of hotter PT is derived to the loss of the other PT in order to expect the thermal balancing effect between the PTs. In other words, if a PT with higher temperature has smaller power loss than the lower temperature PT, then the temperature difference would be reduced. On the other hand, it is supposed that greater power loss in hotter PT would diverge the temperature difference. The relative loss factor of PT is defined as:

$$\Delta P_m = \frac{P_{m2}}{P_{m1}} = \frac{i_{m2}^2 \cdot R_{m2}}{i_{m1}^2 \cdot R_{m1}}, \tag{2}$$

where P_{m1}, P_{m2} are the loss in PT_1, PT_2, respectively. This parameter is used as the index variable to determine whether thermal-balance is achieved or not.

From these parameters, the resonant current (i_m) and power loss on R_m are derived as follows:

$$i_{m1} = \frac{V_m}{Z_{m1}}, \quad i_{m2} = \frac{V_m}{Z_{m2}}$$

$$P_{m1} : P_{m2} = R_{m1}\frac{1}{Z_{r1}^2\left(\frac{1}{\omega_{r1}} - \frac{\omega_{r1}}{\omega_s^2}\right)^2} : R_{m2}\frac{1}{Z_{r2}^2\left(\frac{1}{\omega_{r2}} - \frac{\omega_{r2}}{\omega_s^2}\right)^2} = R_{m1}Z_{r2}^2\left(\frac{1}{\omega_{r2}} - \frac{\omega_{r2}}{\omega_s^2}\right)^2 : R_{m2}Z_{r1}^2\left(\frac{1}{\omega_{r1}} - \frac{\omega_{r1}}{\omega_s^2}\right)^2. \tag{3}$$

When the loss generation on hotter PT is smaller than the other, the PT temperature can converge each other with same radiation of heat. Using this principle, estimate the thermal balance conditions when thermal variation of PT parameter occurs. The methodology is as follows:

– Objective: Derive design parameter range that satisfies the thermal balance condition of parallel–parallel

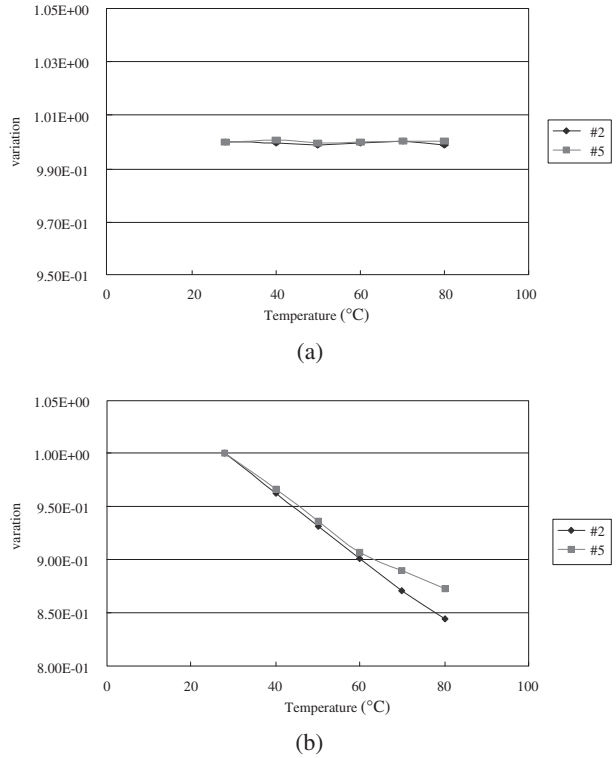

Fig. 6. Resonant frequency and characteristic impedance parameter variation of two PTs (#2 and #5) according to temperature-rise: (a) parameter variation of normalized ω_r ($\omega_{r,Norm} = \omega_{r,temp}/\omega_{r,amb}$) and (b) parameter variation of normalized Z_r ($Z_{r,Norm} = Z_{r,temp}/Z_{r,amb}$).

connection such that the loss of PT_2 is smaller than that of PT_1 ($\Delta P_m < 1$).

– Assumption: There is no difference in every initial parameter values between PT_1 and PT_2 ($\delta X_T = 0$, $\delta X_0 = 0$). PT_2 temperature is higher than that of PT_1.
– Operating condition: ΔX (X: L_{eq}, R_m) is parameter variation rate on the temperature rise.

$$T_{PT2} = T_{PT1} + 10\,^\circ\mathrm{C},\ T_{PT1} = 60\,^\circ\mathrm{C}.$$
$$T_{off} = T_{PT1} - T_{room}(30\,^\circ\mathrm{C}),\ \Delta T = T_{PT2} - T_{PT1}.$$
$$PT_1 : X_1 = X_0(1 + \Delta X \cdot T_{off}),$$
$$PT_2 : X_2 = X_0(1 + \Delta X(T_{off} + \Delta T)).$$

Here, X_0 is the initial parameter value at room temperature (T_{room}), (X_0: $C_{i0}, C_{o0}, L_{eq0}, R_{m0}, N$).

Generally, the mechanical loss of PT are determined by V_m, I_m (the voltage and the current through L_{eq}), and damping resistor R_m. In parallel–parallel structure, since V_m is the same in both PTs when N is identical (practically it is valid among PTs in the same group), the loss is determined only by the variables of L_{eq} and R_m. Because both L_{eq} and R_m decreases according to temperature-rise, it is more desirable for thermal-balance to have greater effect of reduced R_m than that of the current increase from the reduced L_{eq}.

From eqs. (1) and (3), the loss rate in parallel–parallel is derived as eq. (4). By applying the assumption of initial conditions and PT thermal parameters to eq. (4), the objective function ΔP_m is established as eq. (5).

$$P_{m1} : P_{m2} = R_{m1}\frac{1}{{L_{eq1}}^2} : R_{m2}\frac{1}{{L_{eq2}}^2} = R_{m1}{L_{eq2}}^2 : R_{m2}{L_{eq1}}^2$$

where

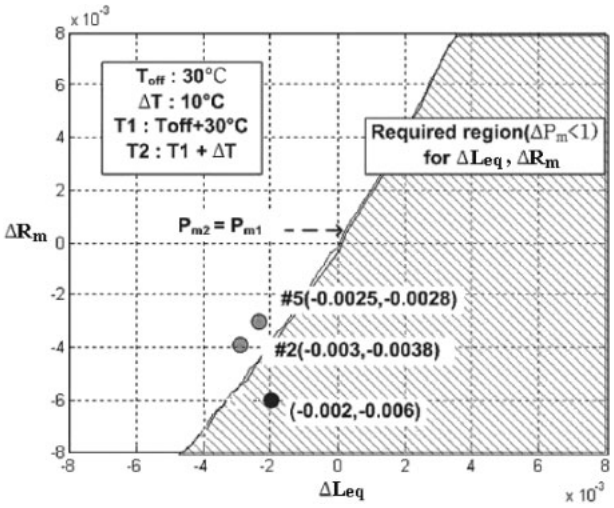

Fig. 7. Design criteria of ΔL_{eq} and ΔR_m for thermal balance and position of some PT examples.

$$R_{m2} = R_{m1}(1 + \Delta R_m \Delta T),\ L_{eq2} = L_{eq1}(1 + \Delta L_{eq}\Delta T) \quad (4)$$
$$\Delta P_m = \frac{1 + \Delta R_m \Delta T}{(1 + \Delta L_{eq}\Delta T)^2} \quad (5)$$

From eq. (5), the design criteria for the thermal balance are derived with ΔL_{eq} and ΔR_m as shown in Fig. 7.

From the results, it is shown that as ΔL_{eq} increases and ΔR_m decreases, PT operation approaches to the thermal balance condition. The figure also shows some examples of 20 W PZT material PT (#2 and #5) implemented by radial vibration mode. Since all the PTs are out of the criteria, the combination of #2 and #5 are thermally unbalance. This design criteria can be verified by the simulation of ΔP_m curves.[6] Figure 8 shows the curves of #2 and #5 combination. The principles of the simulation is presented in previous paper.[6] From the figure, it is shown that ΔP_m is increasing over unity as both the temperature and the temperature gap are increasing. The arrow shows the thermal behavior of the combination. From the analysis, it is supposed that the connection of #2 and #5 are unsuitable for thermal balance. This simulation result corresponds with the hardware result shown in Fig. 3.

3.2 *Design specification of initial deviation of thermal parameter variation according to thermal effect*

Given PTs are unsuitable for the above criteria. Instead of the real devices, a new PT is designated as an acceptable design example of PT, which is the position of (ΔL_{eq}, ΔR_m) = ($-0.002, -0.006$), in required region and close to the real device positions. In this step, we consider the design criteria of acceptable deviation δX_T range of thermal variation parameter.

– Assumptions: ΔX = step A, $\delta X_0 = 0$
– Objective: design criteria of δX_T satisfying $\Delta P_m = P_{m2}/P_{m1} < 1$.
– Operating condition is all the same in previous step but the thermal state definition expressed as:

$$X_1 = X_0(1 + \Delta X \cdot T_{off}),$$
$$X_2 = X_0(1 + (\Delta X + \delta X_T)(T_{off} + \Delta T)), \quad (6)$$

where X: L_{eq}, R_m.

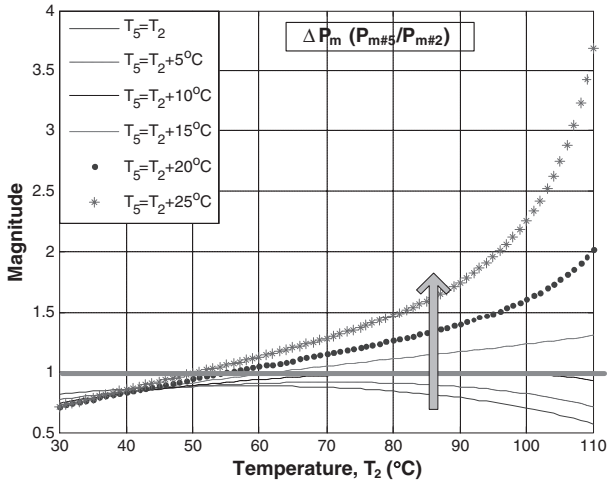

Fig. 8. Thermal behavior simulation of given PT example of #2 and #5 combination in parallel–parallel connection.[5)]

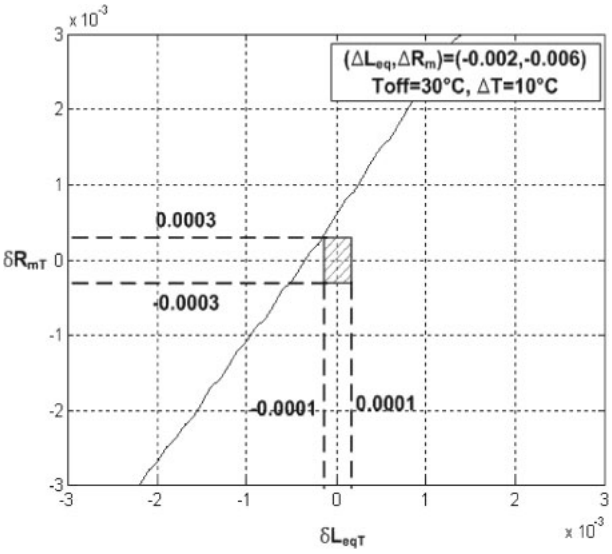

Fig. 9. Design specification of δL_{eqT} and δR_{mT} for thermal balance.

Using eq. (5) and the above operating condition (6), the required region of δL_{eqT} and δR_{mT} is derived shown in Fig. 9.

From the figure, it is shown that the required region is below the line and it is desirable to have greater δL_{eqT} and smaller δR_{mT} for thermal balance. In order to obtain the deviation specification of PT, the design criteria is set as a rectangular area $(\delta L_{\mathrm{eqT}}, \delta R_{\mathrm{mT}}) = (\pm 0.0001, \pm 0.0003)$ as shown in the figure. The worst case is $(\delta L_{\mathrm{eqT}}, \delta R_{\mathrm{mT}}) = (-0.0001, 0.0003)$ and select this point for the next design step.

3.3 *Design specification of initial deviation of thermal parameter according to thermal effect*

In this step, we consider the design criteria of acceptable initial deviation δX_0 of thermal parameters.

- Assumptions: $\Delta X =$ step A, $\delta X_{\mathrm{T}} =$ step B.
- Objective: design criteria of δX_0 satisfying $\Delta P_{\mathrm{m}} = P_{\mathrm{m2}}/P_{\mathrm{m1}} < 1$.
- Operating condition is all the same in previous step but the thermal state definition expressed as:

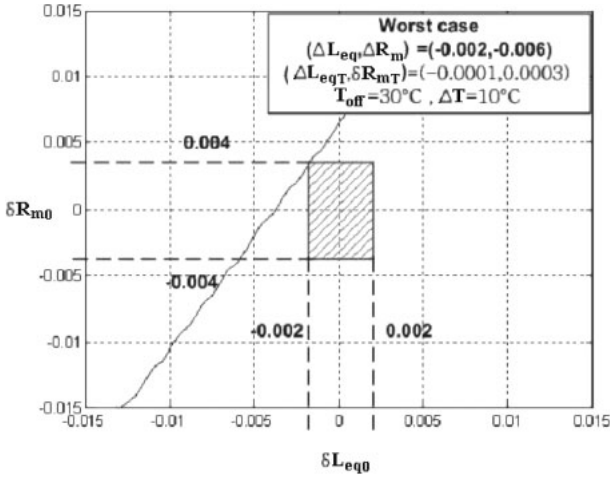

Fig. 10. Design specification of δL_{eq0} and δR_{m0} for thermal balance.

Table II. Worst case example of thermal-balance design criteria.

ΔX	ΔL_{eq}	-0.002
	ΔR_{m}	-0.006
δX_{T}	δL_{eqT}	-0.0001 to 0.0001 ($\pm 5\%$ of ΔL_{eq})
	δR_{mT}	-0.0003 to 0.0003 ($\pm 5\%$ of ΔR_{m})
δX_0	δL_{eq0}	-0.002 to 0.002
	δR_{m0}	-0.004 to 0.004

$$X_1 = X_0(1 + \Delta X T_{\mathrm{off}}),$$
$$X_2 = X_0(1 + (\Delta X + \delta X_{\mathrm{T}})(T_{\mathrm{off}} + \Delta T) + \delta X_0),$$

where X: L_{eq}, R_{m}.

Using eq. (5) and the above operating condition, the required region of δL_{eq0} and δR_{m0} is derived shown in Fig. 10.

From the figure, it is shown that the required region is below the line and it is desirable to have greater δL_{eq0} and smaller δR_{m0} for thermal balance. In order to obtain the deviation specification of PT, the design criteria is set as a rectangular area $(\delta L_{\mathrm{eq0}}, \delta R_{\mathrm{m0}}) = (\pm 0.0002, \pm 0.0004)$ as shown in the figure. The worst case is $(\delta L_{\mathrm{eqT}}, \delta R_{\mathrm{mT}}) = (-0.0002, 0.0004)$.

3.4 *Verification of the PT combination design result*

In this step, we verify the final design result by ΔP_{m} simulation with the worst case. The case is presented in Table II.

The simulation result is shown in Fig. 11. From the figure, it is shown that ΔP_{m} is decreasing under unity as the temperature gap is increasing. The arrow shows the thermal behavior of the combination. From the analysis, it is supposed that even the combination of average and worst PT in a PT group is suitable for thermal balance. If we consider the thermal balance among the worst case combination, PT parameter design spec. (the required region) should be a half.

4. Conclusions

In this paper, design specification of thermal characteristic parameters of piezoelectric transformer in input-parallel and output-parallel connection has been presented for thermal

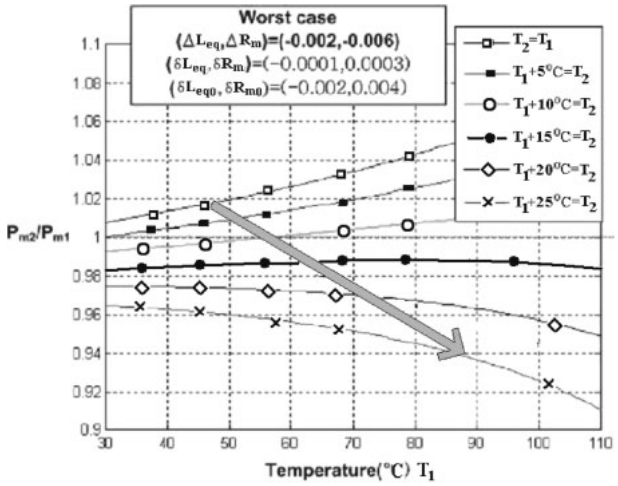

Fig. 11. Thermal behavior simulation of design example with combination of average and worst PT in a PT groups.

balance. In first, the individual thermal characteristics of PT were investigated. It is shown that both the equivalent inductance and resistance in radial vibration mode PTs are reduced with temperature-rise. As an objective function, relative power-loss rate was defined and used for deriving the thermal balance design criteria. The design specification of major design parameters such as thermal parameter variation, deviation parameter of the thermal variation, and initial deviation of thermal parameters are $(\Delta L_{\mathrm{eq}}, \Delta R_{\mathrm{m}}) = (-0.002, -0.006)$, $(\delta L_{\mathrm{eqT}}, \delta R_{\mathrm{mT}}) = (\pm 0.0001, \pm 0.0003)$, $(\delta L_{\mathrm{eq0}}, \delta R_{\mathrm{m0}}) = (\pm 0.0002, \pm 0.0004)$, respectively. Finally, the analysis has been verified by simulation result.

1) M. Yamamoto, Y. Sasaki, A. Ochi, T. Inoue, and S. Hamamura: Jpn. J. Appl. Phys. **40** (2001) 3637.
2) J. Yoo, K. Yoon, Y. Lee, S. Suh, J. Kim, and C. Yoo: Jpn. J. Appl. Phys. **39** (2000) 2680.
3) H. Shin, H. Ahn, and D. Han: J. Power Electron. **3** (2003) 139.
4) S. Choi: Ph. D. dissertation, Seoul National University, Seoul, Korea (2006).
5) S. J. Choi, T. I. Kim, S. M. Lee, and B. H. Cho: PESC05, 2005, p. 624.
6) J. H. Park, S. M. Lee, S. J. Choi, and B. H. Cho: to be published in Int. Symp. Application of Ferroelectrics, 2007.
7) S. Sherrit, G. Yang, H. D. Weiderick, and B. K. Mukherjee: Proc. Int. Conf. Smart Materials: Structure and Systems, 1999, p. 121.
8) T. Endow, S. Hirose, and T. Kanno: Jpn. J. Appl. Phys. **43** (2004) 2976.
9) K. Chang: Jpn. J. Appl. Phys. **43** (2004) 6204.